RECORDS ADMINISTRATION
ABZL

ACC # 727449

DP-MS-81-80

HYDROGEN EFFECTS IN HIGH PURITY STAINLESS STEELS

by

George R. Caskey, Jr.

E. I. du Pont de Nemours & Co.
Savannah River Laboratory
Aiken, SC 29808

SRL RECORD COPY

Accepted for Presentation and Publication
Third International Congress on Hydrogen and Materials
Paris France
June 7-11, 1982

This paper was prepared in connection with work done under Contract No. DE-AC09-76SR00001 with the U.S. Department of Energy. By acceptance of this paper, the publisher and/or recipient acknowledges the U.S. Government's right to retain a nonexclusive, royalty-free license in and to any copyright covering this paper, along with the right to reproduce and to authorize others to reproduce all or part of the copyrighted paper.

7-11/VI/1982

H3

PARIS - FRANCE

TROISIEME CONGRES INTERNATIONAL
HYDROGENE ET MATERIAUX

THIRD INTERNATIONAL CONGRESS
ON HYDROGEN AND MATERIALS

HYDROGEN EFFECTS IN HIGH PURITY STAINLESS STEELS

George R. Caskey, Jr. — Aiken, S.C.

E. I. du Pont de Nemours & Co.
Savannah River Laboratory — USA

RESUME: La fragilization par l'hydrogene gazeux et l'hydrogene interne été étudiée pour aciers inoxydable austénitique (19% Cr et 10, 14 ou 19% Ni) de haut pureté. Les concentrations de C, Mn, Si et P étaient moins de ceux de aciers commercants. Fragilization de aciers haut pureté était comparable avec de acier commercants.

SUMMARY: Internal and environmental hydrogen damage to three pure stainless steels (19% Cr and 10, 14 or 19% Ni) were evaluated by tensile tests. Concentrations of C, Mn, Si and P were less than in commercial alloys. Susceptibility of the pure alloys to hydrogen damage was comparable to that of commercial austenitic stainless steels.

I. INTRODUCTION

Investigations of hydrogen damage to austenitic stainless steels have relied on commercial alloys as the principal source of material for test specimens[1]. In the present study, three stainless steels which contained very low residual concentrations of carbon, phosphorous, silicon and manganese were studied. One objective of this investigation was evaluation of the relative contribution that the common impurities made to hydrogen damage in stainless steels. In addition, austenite stability, which may be a contributing factor to hydrogen damage in austenitic steels, varied among the three alloys because of differences in nickel content. Both environmental and internal hydrogen damage were evaluated with tensile specimens of each alloy.

II. ALLOY CHARACTERIZATION

Smooth bar tensile specimens were machined from three heats of stainless steel made from electrolytic iron, chromium and nickel by vacuum melting and casting. Billets were rolled and swaged to produce 15 mm diameter bars.

The impurity levels in these alloys were substantially lower than in commercial alloys of comparable chromium and nickel contents as seen in Table 1. Tensile specimens were 4.8 mm diameter by 25 mm gauge length. Following machining, all specimens were vacuum annealed two hours at 1170 K and rapidly cooled. The average intercept grain sizes were 19 ± 2 μm, 24 ± 0.6 μm and 25 ± 0.6 μm for alloys A, B and C, respectively.

Microstructures were characterized by equiaxed grains and large chromium-iron carbide inclusions which often occurred in strings or clusters. The carbide inclusions were significantly more frequent as well as larger than in commercial alloys such as Type 304L stainless steel. Alloy A had a duplex-microstructure of 0.5 to 1.0 volume percent ferrite in an austenite matrix.

Segregation was evident in the microstructures of all three alloys following electropolishing and was most pronounced in Alloy C. Samples of both the casting and the rolled and swaged bar of alloy C were analyzed by Scanning Electron Microprobe Quantometer (SEMQ). Alloys A and B were not analyzed. The flow lines corresponded to regions of higher than average chromium and nickel concentration and correspondingly low iron concentration in both the casting and bar. Dendritic segregation during ingot solidification would be expected to produce this segregation pattern for an alloy of 18% chromium and 19% nickel. Dendritic segregation in alloys A and B would not necesarily be the same.

III. EXPERIMENTAL RESULTS

Tensile specimens were pulled to failure at a constant cross head speed of 0.0085 mm/sec. Test environments were air at temperatures of 200 to 400 K and liquid nitrogen at 78 K. Approximately half of the specimens were in the annealed condition whereas the remainder had been saturated with deuterium by exposure to the gas at 69 MPa pressure at 620 K for three weeks.

Deuterium content of samples cut from the tensile specimens was measured with a LECO® (Registered trademark LECO Corporation) RH-1 Hydrogen Determinator. Samples were taken from both the gauge section and the end of the tensile specimens after they had been tested. Average deuterium contents were 52, 116, and 110 ppm (wt) for alloys A, B, and C respectively. The deuterium content of alloy A was less than for Type 304L stainless steel for the same exposure conditions. The other two alloys dissolve substantially more deuterium than Type 304L stainless steel. Samples cut from the deformed gauge portion of the tensile specimens of alloy A contained less deuterium than the end samples, an effect that was more pronounced at lower test temperatures.

III.1. Internal Hydrogen Effects

Strength and ductility of all three alloys (Table 2) were comparable to the properties of 300 series stainless steels of similar composition. In the case of alloy A, strength increased continuously with lowering temperature. In contrast, the yield strengths of alloys B and C were highest at intermediate temperatures, 200-270 K.

The nickel content of the alloys had a pronounced effect on the temperature dependence of ductility for the hydrogen charged specimens. Ductility minima were observed in alloys A and B at 230 K but not in alloy C. Furthermore, the ductility minimum in alloy A was substantially broader than in alloy B. Figure 1 depicts the temperature - ductility - nickel relationship for these alloys. All specimens were checked for the presence of α'-martensite with a ferrite indicator both near the fracture and at the ends where no significant deformation occurred. Alloy A transforms

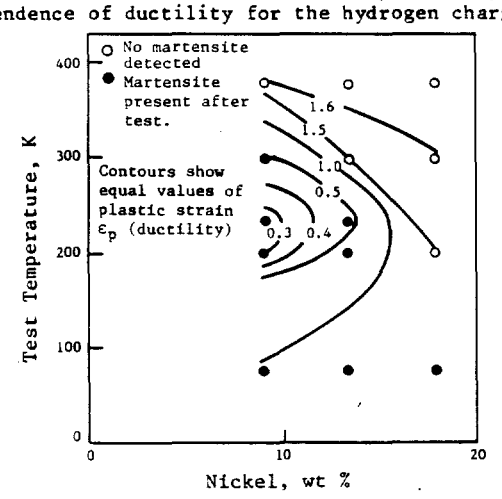

FIGURE 1. Isoductility Diagram for Hydrogen-Charged Fe-Cr-Ni Alloys

partially to martensite upon cooling below 200 K, so that the specimen tested at 78 K contained some martensite prior to deformation. Nonetheless this specimen was nearly as ductile as the companion which did not contain any hydrogen.

The temperature and composition dependences of the mechanical properties of the pure alloys parallel those of commercial alloys[1]. Alloys with low nickel content (<12%) have a hydrogen induced ductility minimum at about 200-250 K. As the nickel content increases, the ductility minimum disappears. Furthermore, the hydrogen induced ductility loss is associated almost entirely with necking strain, as measured by reduction area, for example. Uniform elongation is only slightly reduced by hydrogen. These observations imply that the impurity content (phosphorus, silicon, carbon and manganese) of the commercial alloys does not control the nature of extent of hydrogen damage as measured by loss of tensile ductility.

Evaluation of susceptibility to hydrogen damage of an alloy depends not only on the magnitude of the property change but also upon the quantity of hydrogen required to effect that change. Alloy A dissolved only 40% as much hydrogen as either Alloy B or C for the same exposure conditions. Therefore, comparison of the alloys on the basis of equal concentrations of dissolved hydrogen accentuates the differences in hydrogen damage among the alloys. For example, losses in ductility due to hydrogen for tests at 200 K are 23%, 5.4%, and 0.15%, respectively, for Alloys A, B, and C when normalized to unit hydrogen concentration.

III.2. Fractography

On a macroscopic scale all failures were cup-cone fractures except for the three specimens of alloy A and two specimens of alloy B which were tested within the region of maximum hydrogen damage. These five specimens failed with a flat rough fracture which gave little evidence of neck formation.

The dominant microscopic fracture mode was microvoid coalescence (Figure 2a). This was the only fracture mode observed in specimens which were free of hydrogen and also appeared in all specimens that contained hydrogen. Dimple size distributions were not measured; therefore, it is not certain if hydrogen affected dimple growth as observed in other stainless steels[2].

Twin boundary parting (Figure 2b) is the characteristic fracture mode in hydrogen charged Type 304L stainless steel at 200-270 K[3]. Facets similar to those in Type 304L stainless steel were observed in specimens of alloy A tested at 200 and 235 K but not in the specimen tested to 298 K. Facets were seen also

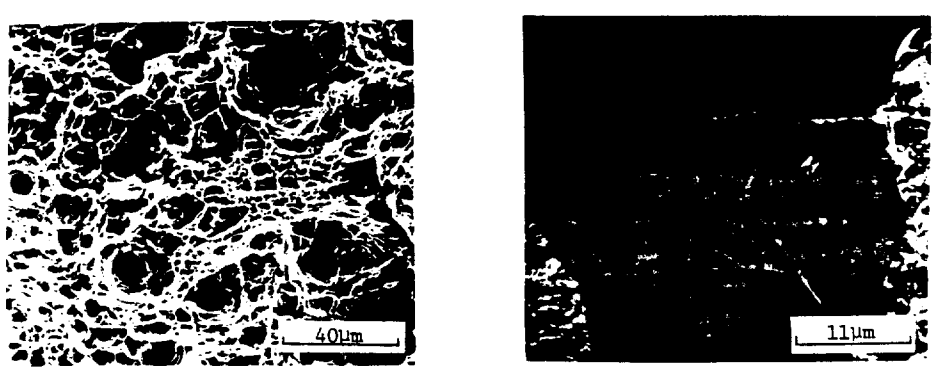

a) Microvoid coalescence. b) Twin boundary parting.

FIGURE 2. Microscopic Fracture Modes

in the specimen of alloy B tested at 235K but they were less frequent than in alloy A. In general, facets observed in these high purity alloys were not as sharply delineated as in Type 304L stainless steel, but they did possess the same characteristics[3].

Microcracks transverse to the tensile axis were observed on longitudinal sections cut from the gauge sections of the specimens that showed facets on their fracture faces, Table 3. Microcracks were not seen in shoulder or end sections of the specimen. As in other stainless steels, the microcracks do not propagate from one grain to the next[3]. Crack frequency correlated with facet frequency. Microcracks near the fracture surface had a wider opening than cracks distant from the fracture.

III.3. Environmental Hydrogen Effects

Susceptibility of the alloys to hydrogen environment embrittlement was examined by testing pairs of specimens of each alloy in high pressure (69 MPa) helium or hydrogen at room temperature. The only specimen that showed reduced ductility was the specimen of Alloy A tested in hydrogen, Table 4. The fracture was flat with some longitudinal cracking and a crystallographic appearance over a large portion of the fracture as shown in Figure 3. A longitudinal metallographic section through the fracture showed evidence for secondary cracking along grain boundaries. Elongated islands of ferrite were observed in alloy A in association with boundaries. Areas of crystalline appearance are similar to fractures in unstable austenitic steels that have been attributed to failure in strain induced martensite or along austenite-martensite interfaces[4].

IV. DISCUSSION

Impurities in austenitic stainless steels may affect their susceptibility to hydrogen damage by segregating to internal boundaries or by changing the austenite stability. Impurity segregation was not expected in the present case because of low impurity concentrations and the annealing treatment at 1170 K. The only evidence of intergranular fracture was in the specimen of alloy A tested in high pressure hydrogen. Ferrite was associated with grain boundaries in alloy A and probably provided an easy fracture path as in welds in Type 304L stainless steel[5]. The ferrite is not caused by impurity segregation but rather by chromium, nickel and iron segregation.

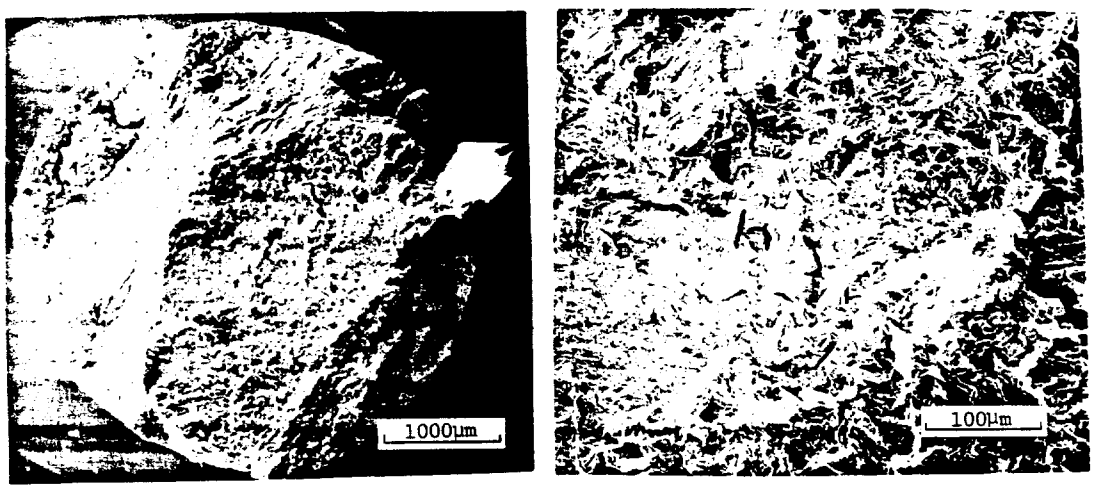

FIGURE 3. Fracture in Hydrogen Gas. Alloy A.

Hydrogen damage in metastable austenitic steels, such as alloys A and B, has been attributed to strain-induced martensite[6]. In those specimens where hydrogen damage was large, strain-induced martensite had formed. However, several other specimens also developed large amounts of strain-induced martensite with little or no hydrogen damage. Consequently, martensite per se does not render an austenitic steel highly susceptible to hydrogen damage. This observation has been made with other austenitic steels also[1]. The common factors among those austenitic steels which are highly susceptible to internal hydrogen damage are the temperature (200-250 K) where the damage is greatest and the occurrence of the twin boundary parting fracture mode.

V. ACKNOWLEDGEMENTS

This paper was prepared in connection with work done under Contract No. DE-AC09-76SR00001 With the U.S. Department of Energy. Alloys in this study were supplied by N. F. Fiore, University of Notre Dame.

REFERENCES

[1] CASKEY G.R., Hydrogen damage in stainless steel. Environmental Degradation of Engineering Materials, ed., M. R. Louthan, R. P. McNitt and R. D. Sisson. Virginia Polytechnic Institute, Blacksburg, VA., (1981), 283-302.

[2] THOMPSON A. W., The Mechanism of hydrogen participation in ductile fracture. Effect of Hydrogen on Behavior of Materials, ed. A. W. Thompson and I. M. Bernstein. Metallurgical Society of AIME, New York, NY (1976), 467-477.

[3] CASKEY G.R., Hydrogen-induced brittle fracture of Type 304L austenitic stainless steel. Fractography and Material Science, ASTM STP 733, American Society for Testing and Materials, Philadelphia, PA (1981), 86-97.

[4] ELIEZER, D. - CHAKRAPANI D.G. - ALTSTETTER C. J. - PUGH E.N., The influence of austenite stability on the hydrogen embrittlement and stress-corrosion cracking of stainless steel. Met. Trans. 10A (1979), 935-941.

[5] WEST A.J. - BROOKS J. A., Hydrogen compatibility of 304L stainles steel welds, Effect of Hydrogen on Behavior of Materials, ed., A. W. Thompson and I. M. Bernstein, Metallurgical Society of AIME, New York, NY (1976), 686-697.

[6] BENSON, R. B., DANN, R. K., and ROBERTS, L. W., Hydrogen embrittlement of stainless steels. Trans ASM 24, (1968), 2100-2205.

TABLE 1

Alloy Compositions

Alloy	C	Mn	P	S	Si	Cr	Ni	Al	N	O
A	0.01	<0.01	<0.005	0.015	0.04	17.87	10.03	0.008	0.005	0.046
B	0.01	<0.01	<0.005	0.007	0.03	17.64	14.35	0.005	0.012	0.051
C	0.01	<0.01	<0.005	0.010	0.04	17.75	18.83	0.10	0.009	0.038
304L*	0.03	1.57	0.015	0.008	0.43	18.35	10.29	-	-	-

* Typical heat analysis

TABLE 2

Mechanical Properties

Test Temp., K	Strength MPa Yield	Strength MPa Ultimate	Elongation % Uniform	Elongation % Total	Fracture Strain
Alloy A					
370	230	610	45	52	1.57
	270*	660	60	59	1.65
298	350	1270	62	73	1.66
	290*	1030	60	60	0.50
235	390*	1110	38	38	0.27
200	540	1320	36	46	1.42
	420*	1190	33	33	0.31
78**	-	1010	40	47	1.16
	-	1060	42	48	1.13
Alloy B					
370	240	630	45	56	1.58
	260*	660	46	56	1.40
298	340	1020	61	69	1.56
	290*	870	65	72	1.50
235	320*	1170	72	79	0.44
200	340	1170	64	74	1.57
	380*	1250	66	71	0.89
78**	260	870	63	67	1.37
	270*	900	66	72	1.41
Alloy C					
370	250	630	44	52	1.62
	260*	660	45	53	1.45
298	330	910	49	58	1.65
	290*	770	52	62	1.55
200	300	1100	78	87	1.52
	330*	1170	78	86	1.50
78**	250	850	82	89	1.53
	280*	890	80	86	1.43

* Hydrogen charged at 69 MPa pressure.

** Tested in liquid nitrogen.

TABLE 3

Frequency Of Microcrack Occurrence

Alloy	Test Temp., K	Crack Frequency Cracks/mm^2
A	298	1.94
	235	21.00
	200	7.60
B	235	1.85
	200	1.23
C	(no microcracks)	

TABLE 4

Effect Of High Pressure Gas On Tensile Ductility

Alloy	Fracture Strain Helium	Fracture Strain Hydrogen
A	1.72	0.30
B	2.77	2.42
C	1.71	2.48